Virtual Prototyping of a floating wind farm anchor during underwater towing operations *

Rodrigo Martinez[1], Sergi Arnau[1], Callum Scullion[2], Paddy Collins[2], Richard D. Neilson[1], and Marcin Kapitaniak[1]

[1] The National Decommissioning Centre, School of Engineering, University of Aberdeen, UK
[2] Aubin Group, Castle Street, Castlepark Industrial Estate, Ellon AB41 9RF, UK

Abstract. The aim of this paper is to present the initial results of feasibility studies aimed at optimising the towing configuration of a novel, complex shape (pyramid based) and thereby untested design of floating wind farm anchor during underwater towing. The study was carried out in the real physics Marine Simulator, at the National Decommissioning Centre. This enables us to study in detail, the drag/lift forces acting on the towed anchor/s, determine the optimal anchor installation arrangement (orientation, depth, position of towing cables, number of anchors towed together in an array) and establish the effects of the operational (towing velocity, drag) and environmental conditions (sea states, significant wave height, peak wave period) on the anchor's trajectory. The model developed is validated with computational fluid dynamics analysis to obtain representative drag and lift coefficients for the anchor during towing. Thus, this paper focuses on the calibration process to ensure robustness and relevance of the developed model in the simulator. Consistent results for the drag and lift coefficient were obtained for a range of towing speeds (0,25-3 m/s). The towing dynamics, forces acting on the anchor and the final configuration (e.g. water depth, offset angle) were obtained which in turn will allow the optimal conditions and requirements (e.g. equipment, vessel type etc.) to be recommend-ed in future studies.

Keywords: Marine simulator · Virtual Prototyping · Underwater towing operation · Anchor · Floating wind farm

1 Introduction

Novel installation methods of anchors for offshore wind are currently being developed worldwide. Four of the most common floater types of offshore wind are shown in Figure 1: semi-submersible, spar-buoy, tension-leg platform (TLP) and barge [1]. All four types of floating wind structures use mooring and anchoring systems to keep the structure in place. A state-of-the art review of the installation

---

phase of offshore wind turbines is presented in [6,7,4]. Various installation methods for floating wind are critically discussed and the main challenges identified. It is concluded that the complex anchoring systems used presently are expected to evolve with new foundations technologies. A technology review conducted by Jiang [7] also concludes that considerable CapEx and OpEx savings are possible from developing and optimising new mooring and anchoring systems.
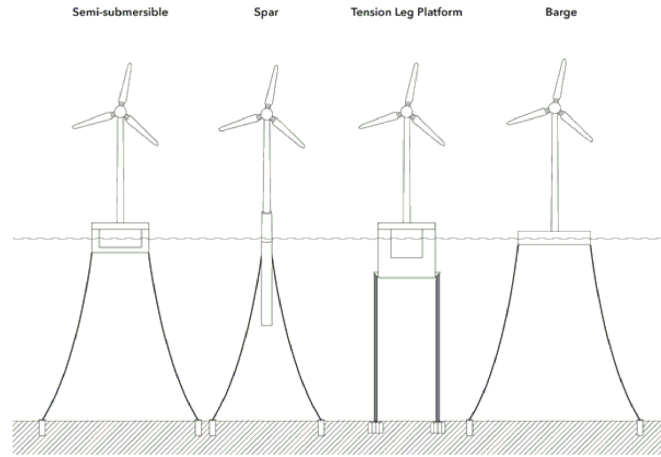

Fig. 1: Four common floater types for wind turbines [6]

In addition to optimising the installation process of anchors, Jiang [7] also identifies the need to develop new advanced modelling software to accurately simulate coupled behaviours of floating wind systems. In this context, the simulator at the National Decommissioning Centre (NDC) has been used to conduct virtual field trials, with the aim to prototype new installation method of anchors for offshore wind, with a primary focus on the installation challenges of floating wind farm anchors and mooring systems [10]. This will lead to the development of novel techniques for the deployment of wind farm anchors and mooring systems, which will be tested comprehensively through simulation of different scenarios to establish the applicability of the proposed methods in various weather conditions, sea states and ultimately study their benefits and limitations. This research will in turn enable a wider range of vessels (lower cost/less specialist) during anchorage/mooring installation and increased precision of the installation of the sub-sea equipment which could lead to the reduction of costs and CO_2 emissions.

In this study, the feasibility of an underwater towing operation that involves a novel type of anchor with variable buoyancy for mooring floating offshore wind turbines is presented (Figure 2a). The proposed system reduces the need to use a Heavy Lift Vessels (HLV), thereby cutting overall installation costs, and reduces

the installation lead times as the design of the operation is less dependent on sea and weather conditions. In this context, the industry is continuing to minimise installation costs by developing self-installing and port assembled systems.
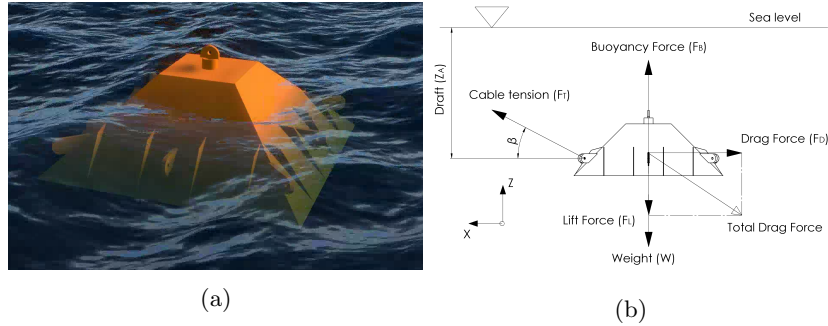

(a)

(b)

Fig. 2: (a) 3D render of the novel floating anchor concept. (b) free body diagram of the anchor.

A set of detailed modelling studies are performed in the state-of-the-art, Marine Simulator at the NDC. Using the multi-physics simulation allows for a more economical proof-of-concept approach, that will allow to fully assess the feasibility of underwater towing of anchors and de-risk future offshore deployment operations.

2   Virtual prototyping

A review of virtual prototyping (VP) of offshore operations can be found in [9]. The importance of working with a tool that can integrate the different project phases from concept/tender, engineering, mobilisation, through operations is vital for future offshore operations to reduce cost and minimise risks. An example of virtual prototyping using the marine simulator supplied by the Offshore Simulator Centre (OSC) is presented in [11]. In this example, the real-time VP model is used to simulate the process of a riser pulled in from an installation vessel to a jacket platform. With special attention being made to the maximum bending curvature along the flexible riser, as this is one of the critical aspects during the operation. Finally, the results are validated against finite element (FE) analysis resulting in good agreement. Another example study stating the importance of simulations based on multi-body dynamics is presented in [8], in which a comprehensive analysis of potential collisions between objects during offshore lifting operations is made.

The study for a new concept of transportation of sub-sea templates is presented in [5], in which an underwater towing method is proposed. In this study, the dynamical effects involved during the towing operations are discussed and

analysed by means of: (1) a mathematical mass-spring model with forced exci-
tation, (2) a multi-body time domain simulation using the software SIMO [2]
and (3) a physical model test in the laboratory. A good agreement was found
between the three methodologies, specially between the SIMO analysis and the
experimental results. Another example to study the underwater towing of a sub-
sea module is presented in [12], in which the results of a computational fluid
dynamics (CFD) model are compared with experimental results. Gu et al. [3]
presents a study of a large caisson during wet-towing transportation. The cais-
son resistance coefficient was simulated via Ansys Fluent software and resultant
CO_2 emissions under various conditions were calculated.

3   Methodology

3.1   Test Set-up

To investigate the variation of the towing force (drag and lift force) with the tow-
ing velocity, a set of simulations using both marine simulations and CFD analysis
using Ansys Fluent are conducted. The parameters used in both simulations are
shown in Table 1.

Table 1: CFD parameters

Case	Speed (m/s)	Angle of Attack (deg)	Fluid
1	0.25	0	sea water
2	0.50	0	sea water
3	0.75	0	sea water
4	1.00	0	sea water
5	1.25	0	sea water
6	2.00	0	sea water
7	3.00	0	sea water

Towing direction: +X (see Figure 3)

The model remains underwater at all times (wet towing). The general di-
mensions of the anchor are 10 m wide, 10 m long and 3,48 m high and it has
a truncated pyramid shape as indicated in Figure 2b. The length of the towing
line is 22.1 m and the wet weight of the anchor for this set of simulations is
10.5 kN. Further information on the methodology used to carry out the marine
simulations can be found in [10].

3.2   Physical Model

The free body diagram of the anchor with submerged weight W, buoyancy force
F_B, towing force F_T, hydrodynamic drag F_D and lift F_L forces and offset angle
β is shown in Figure 2b. In the steady state, the system can be simplified to

Equation 1 and 2, where the weight and drag force of the wire have been ignored. At any given vertical position Z_A, the system satisfies the following equilibrium in the Y and Z directions (see Figure 3)

$$F_T \cos \beta - F_D = 0, \tag{1}$$

$$F_T \sin \beta + W - F_L = 0. \tag{2}$$

3.3   CFD

To verify the results obtained in the marine simulator, a series of CFD simulations in Ansys Fluent are carried out to determine the drag and lift coefficient for a range towing speeds (0,25-3 m/s) and at an angle of attack of 0°. Furthermore, a detailed study of the flow field is made to visualise the vortex pattern around the anchor during towing.

Figure 3 shows the computational domain used in the simulations. The leading edge of the anchor is 1L away from the velocity inlet and the aft is 3L away from the pressure outlet. In addition, the lateral, top and bottom distance between the anchor and the walls is 1L, 1.5L and 1L, respectively. In this case, the characteristic length L is 10 m. Each case was simulated using the Reynolds-Average Navier-Stokes equation (RANS) method. In the current work, the k-ω STT turbulence model was applied. The mesh size is selected so that the simulation produces consistent results regardless of the size and the number of cells yet producing results efficiently. The inflation layer meshing technique is used around the anchor to capture the boundary layer in the near-wall region. The resistance created by the towing rope is not included in the CFD simulation, as it is considered to be small in comparison to the drag force.
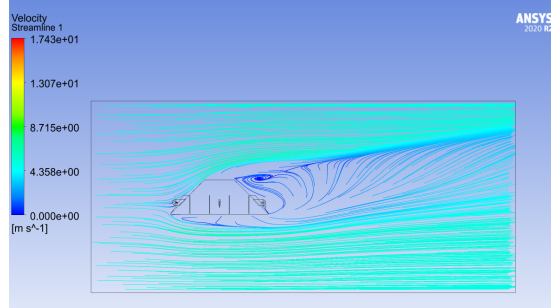

Fig. 3: CFD simulations flow velocity streamlines around the submerged anchor.

The output of each simulation was the drag force in the direction of the flow (X) and the lift force, perpendicular to the direction of the flow (Z). Once the drag and lift force have been obtained for each scenario, they can then be used

to calibrate the marine simulations. For each CFD analysis, the drag and lift coefficient are determined as:

$$C_D = \frac{2F_D}{\rho A V^2}, \tag{3}$$

$$C_L = \frac{2F_L}{\rho A V^2}, \tag{4}$$

where F refers to the drag or lift force, ρ is the density of sea water, A is the area of body incident to flow, and V is the velocity at which the vessel is moving.

3.4 Marine simulator

The towing system consists of a tugboat, the new anchor model and a towing rope, as shown in 4. For this preliminary study, the calibration was done during the steady-state stage of towing to minimise the effects of acceleration and with a calm sea (e.g. without waves, wind and currents). In this stage, the vessel and the anchor have a constant speed and the anchor's position in the water column and its orientation (e.g. pitch, role and yaw) are also constant. This creates a scenario as close as possible to the one simulated in Ansys Fluent, at which point the results of the CFD analysis can be used to calibrate the marine simulator. Martinez et al. [10] describes the process and methodology to setup a simulation in the state-of-the-art marine simulator.
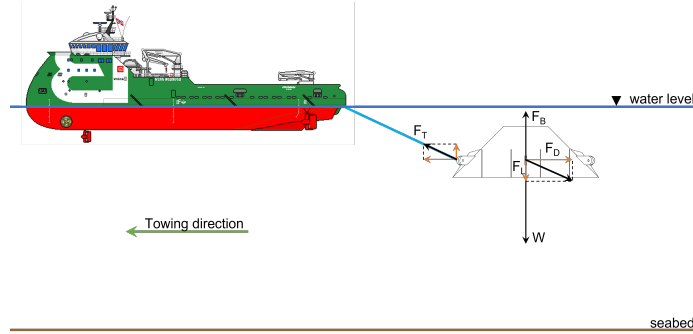

Fig. 4: Representation of the towing operation in the marine simulator.

4 Results

In this section, the results presented are divided in two sections: CFD simulations for which the drag coefficient C_D was calculated and, marine simulations in which the previously calculated C_D serves as an input to analyse the towing operations under different wave conditions and length of tow lines.

4.1 CFD simulations

Figure 3 shows the flow velocity streamlines around the anchor when being towed at $v = 3.0$ m/s speed. Flow separation and vortex generation at the back of the anchor is observed.

Figure 5 (a) shows the calculated drag (blue) and lift (red) forces for different towing speeds while keeping the anchor horizontal. Drag and lift coefficients, C_D and C_L respectively, are then calculated using Equations 3 and 4. These values are then used as calibration input on the marine simulator. This process is performed for each towing scenario to get realistic drag and lift force data from the simulator.

4.2 Marine simulations

Once the drag and lift coefficients are calibrated, the towing operations are tested in the marine simulator.

The variation of the calibrated drag and lift forces with towing speed are shown in Figure 5 (b). The blue line is the drag force and the red line is the lift force. Green markers represent tests done with tow line length $L_{tow} = 22.1$ m, blue markers $L_{tow} = 41.6$ m and black markers $L_{tow} = 60.2$ m. From the figure it can be seen that, regardless of the tow line length, their respective drag and lift forces behave similarly at all towing speeds.

Figure 5 (c) shows the depth at which the anchor settles at all towing speeds for the three tow line lengths with same colour code as Figure 5 (b). Although the tow line length does not have an impact in the drag and lift forces, it does have an impact on the depth (Z_A) at which the anchor is being towed. At lower towing speeds, the anchor sinks the furthest and at higher speeds the anchor gets closer to the surface. The length of the tow line is directly proportional to the equilibrium depth of the anchor: the longer the tow line, the deeper the anchor is being towed and the shorter the tow line, the closer to the water surface the anchor is being towed.

Next, for a fixed significant wave height of $H_S = 2.03$ m, parametric studies varying the peak wave period T_P are performed to establish the effect of wave loading on the towing dynamics, as shown in Figure 6. In here, we consider only single tow line length of $L_{tow} = 22.1$ m, under towing velocity of $v = 1$ m/s and JONSWAP wave spectrum ($\gamma = 3.3$). Waves with $T_P < 4$ s have no noticeable effect on the anchor's position and orientation and towing force. For $T_P > 4$ s, wave-induced oscillations are more visible, maximum values for force and anchor depth amplitude are reached at $T_P \approx 15$ s. Yaw presents a local minima at $T_P \approx 5$ s, after which, its values start moving back to 0°. Pitch and roll, however, have a local minima at $10 < T_P > 11$ s.

Figure 7 shows example time histories for the anchor's dynamic response for towing with $T_P = 5.5$ s. In each of the time histories there is steady state response of regular periodic type (27 periods of excitation are plotted). Right hand side panels show the corresponding phase portraits that show the orbit of the response for each of the anchor parameters. Once the anchor reaches
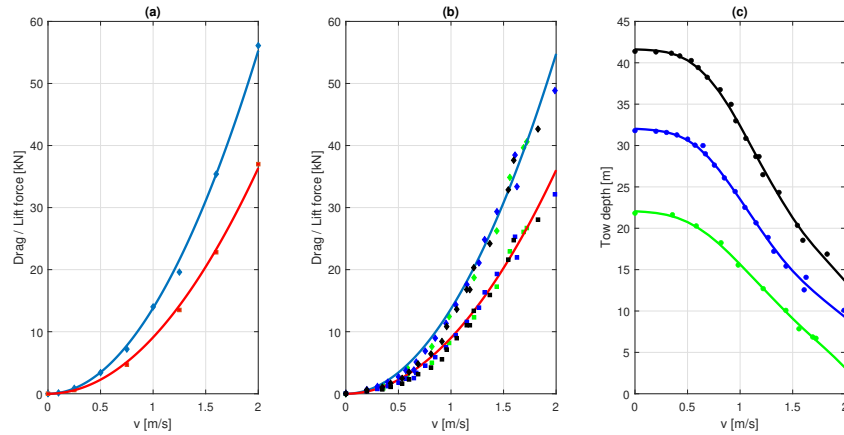
Fig. 5: (a) Drag and lift forces as a function of flow velocity from CFD analysis, (b) Calibrated response for towing drag and lift forces obtained from developed simulation for tow line lengths of $L_{tow} = 22.1$ m (green markers), $L_{tow} = 41.6$ m (blue markers), $L_{tow} = 60.2$ m (black markers), (c) The equilibrium tow depth of the anchor as a function of towing velocity for tow line lengths of $L_{tow} = 22.1$ m (green), $L_{tow} = 41.6$ m (blue), $L_{tow} = 60.2$ m (black).

an equilibrium, its pitch, towing force and anchor depth reach a stable orbit (period-2), that show the maximum/minimum variation of these quantities and their corresponding velocities.

5   Conclusions

The towing feasibility of a novel floating anchor design is described in this work. CFD simulations are initially performed to calculate drag and lift coefficients that would serve as input for realistic simulations in the marine simulator.

The analysis performed in the marine simulator shows that during towing operations, the drag and lift forces are not impacted by the length of the tow line. The towing depth of the anchor decreases as the towing speed increases but the towing depth of the anchor increases as tow line length increases. Simulations also show that wave period has a large impact in the anchor's depth and towing force at $T_P \approx 15$ s and at $T_P \approx 5$ s on the anchor's orientation (pitch, roll and yaw).
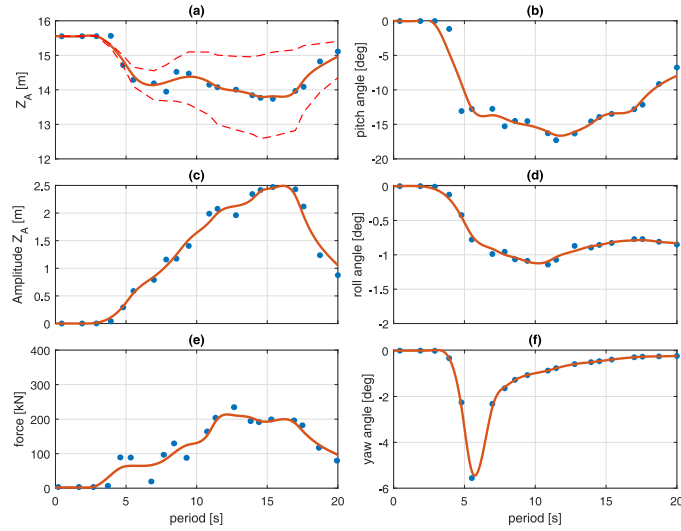
Fig. 6: Parametric plots depicting the effect of wave period on the anchor towing dynamics (using towing line of length L_{tow} = 22.1 m) for (a) anchor vertical position Z_A (dashed lines mark the min/max values), (b) amplitude of anchor's vertical position, (c) towing force, amplitude of anchor's pitch (d), roll (e) and yaw (f) angles.
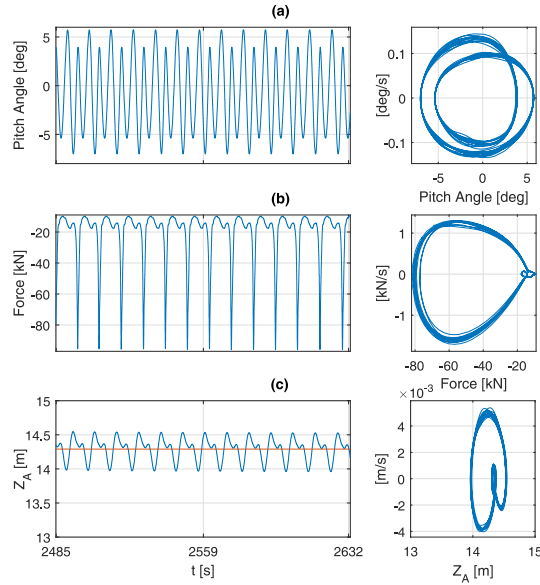

Fig. 7: An example of family of time histories for (a) anchor's pitch angle, (b) towing force, (c) anchor's vertical position Z_A and corresponding phase portraits (right panels) depicting anchors dynamics for peak wave period of T_P = 5.5 s

References

1. DNV-GL: DNVGL-ST-0119 - Floating wind turbine structures (2018), https://rules.dnv.com/docs/pdf/DNV/ST/2018-07/DNVGL-ST-0119.pdf
2. DNV-GL: Feature Description: Sesam. Software suite for hydrodynamic and structural analysis of renewable, offshore and maritime structures (2022), https://www.dnv.com/Images/Sesam-Feature-Description_tcm8-58834.pdf
3. Gu, H., Wang, H., Zhai, Q., Feng, W., Cao, J.: Study on the dynamic responses of a large caisson during wet-towing transportation. Water (Switzerland) **13** (1 2021). https://doi.org/10.3390/w13020126
4. Ikhennicheu, M., Lynch, M., Doole, S., Borisade, F., Matha, D., Dominguez, J.L., Vicente, R., Tim, H., Ramirez, L., Potestio, S., Molins, C., Trubat, P.: Review of the state of the art of mooring and anchoring designs, technical challenges and identification of dlcs. Tech. rep., COREWIND (2020)
5. Jacobsen, T., Leira, B.J.: Numerical and experimental studies of submerged towing of a subsea template. Ocean Engineering **42**, 147–154 (2012). https://doi.org/10.1016/j.oceaneng.2012.01.003
6. James, R., Ros, M.C.: Floating offshore wind: Market and technology review. Tech. rep., The Carbon Trust (2015), https://www.carbontrust.com/resources/floating-offshore-wind-market-technology-review
7. Jiang, Z.: Installation of offshore wind turbines: A technical review. Renewable and Sustainable Energy Reviews **139**, 110576 (2021). https://doi.org/https://doi.org/10.1016/j.rser.2020.110576
8. Lee, H.W., Roh, M.I.: Review of the multibody dynamics in the applications of ships and offshore structures. Ocean Engineering **167**, 65–76 (2018). https://doi.org/https://doi.org/10.1016/j.oceaneng.2018.08.022
9. Major, P., Zhang, H., Hildre, H.P., Edet, M.: Virtual prototyping of offshore operations: a review. Ship Technology Research **68**(2), 84–101 (2021). https://doi.org/10.1080/09377255.2020.1831840
10. Martinez, R., Arnau, S., Scullion, C., Collins, P., Neilson, R.D., Kapitaniak, M.: Deployment feasibility studies of variable buoyancy anchors for floating wind applications. Mechanisms and Machine Science (2022), [Accepted]
11. Yuan, S., Major, P., Zhang, H.: Flexible riser replacement operation based on advanced virtual prototyping. Ocean Engineering **210**, 107502 (2020). https://doi.org/https://doi.org/10.1016/j.oceaneng.2020.107502
12. Zan, Y., Guo, R., Yuan, L., Wu, Z.: Experimental and numerical model investigations of the underwater towing of a subsea module. Journal of Marine Science and Engineering **7** (2019). https://doi.org/10.3390/jmse7110384